



DOI: 10.18720/MCE.90.1

Structure, composition and properties of geopolymers from mineral wool waste

V.T. Erofeev, A.I. Rodin*, V.V. Yakunin, M.N. Tuvin

Ogarev Mordovia State University, Saransk, Respublika Mordoviya, Russia

* *E-mail: al_rodin@mail.ru*

Keywords: geopolymers, slags, mineral wool, mechanical properties, X ray diffraction analysis, thermoanalysis, microstructure

Abstract. The waste generated during the mineral wool production makes up to 30 % of the finished product mass. These wastes can be used for producing building materials, in particular as raw materials for the production of geopolymers (alkali-activated binders). The research aim was to determine the influence of the chemical composition of mineral wool production wastes (MWPW) on the phase composition, structure, and physico-mechanical properties of geopolymers. Five types of MWPW with various chemical compositions and specific surfaces were hydrated in the presence of NaOH (from 2 to 4 wt. %). The experimental results were obtained using the methods of X ray differential (XRD), differential thermal (DTA) and thermogravimetric (DTG) analyses. Moreover, scanning electron microscopy (SEM) and physical and mechanical tests were used. The main hydration product of MWPW in the NaOH presence is determined to be calcium hydrosilicates of the C–A–S–H fiber texture type. The largest amount of C–A–S–H was detected in geopolymer samples made of wastes with an acidity modulus between 1.4 and 1.6. The compressive strength of the obtained materials reaches 80 MPa. They are also characterized by high water resistance. The Al_2O_3 content in the waste should be about 10 % in order to obtain geopolymers with stable properties. The obtained results made it possible to define the correlation between the structure, composition, and physico-mechanical properties of geopolymers made of MWPW. The practical effect of the research results lies in the possibility of obtaining higher strength classes concrete.

1. Introduction

One of the most popular material types in modern construction are cement binders. Alkali-activated binders (geopolymers) can become a good alternative to them. Materials based on them possess high strength and chemical resistance. Implementing such materials also helps to solve environmental problems; it helps to reduce CO_2 emissions into the atmosphere, reduces pollution of surface waters and groundwater, atmosphere, soil and plants [1–6]. The technology for producing geopolymers is as follows. Slags of metallurgical industries are milled to the specific surface of Portland cement and tempered with alkaline solutions. The most of construction products and structures based on alkali-activated binders are obtained using blast furnace slag of iron industry. Slags of non-ferrous metallurgy, furnace clinkers (ashes), chemical and a number of others are also widely used [7–13]. A special category of slag includes mineral wool production waste (MWPW). Up to 30 % of such waste from the mass of finished products is generated during production process [14]. The possibility of using MWPW in order to obtain geopolymers was described before [14].

Analyzing the mineral wool chemical composition of the most famous world manufacturers (ROCKWOOL, Knauf, etc.) showed that the CaO content in most samples is between 20 and 30 %, and the total amount of Al_2O_3 and MgO is more than 20 %. Understanding the correlation between the chemical composition of MWPW and physico-mechanical properties of hardened composites is possible only through a comprehensive study of the hydration processes in waste activated by alkaline solutions. Such studies are almost absent in the literature. However, hydration processes of blast furnace slag with various chemical compositions, tempered with silicate or alkali metal hydroxide solutions, have been studied quite extensively [2, 15–19]. It is known that the main product of this interaction is a calcium hydrosilicate gel of the C–A–S–H type. The structure of this gel is similar to tobermorite with a partial replacement of Ca by Al. According to studies [15, 18], this structure is characterized by a higher polymerization degree, as well as a greater degree

Erofeev, V.T., Rodin, A.I., Yakunin, V.V., Tuvin, M.N. Structure, composition and properties of geopolymers from mineral wool waste. Magazine of Civil Engineering. 2019. 90(6). Pp. 3–14. DOI: 10.18720/MCE.90.1

Ерофеев В.Т., Родин А.И., Якунин В.В., Тувин М.Н. Структура, состав и свойства геополимеров из отходов минеральной ваты // Инженерно-строительный журнал. 2019. № 6(90). С. 3–14. DOI: 10.18720/MCE.90.1



of crosslinking between tobermorite chains. Many researchers [2, 15, 18, 20–26] argue that secondary phases, such as zeolites and the N–A–S–H gel, are formed in the composition of CaO and MgO when hydrated, in addition to the C–A–S–H gel; hydrotalcite is formed in case of high CaO and MgO content; sterlinghillite is formed in case of high Al₂O₃ and CaO content; and etc.

The ratio of oxides in the slag is of particular importance for the formation of both the C–A–S–H phase and secondary phases during hydration of alkali-activated binders: CaO/SiO₂, MgO/Al₂O₃ and Al₂O₃/SiO₂. According to studies [2, 18, 19, 22, 25, 27], the increased CaO content in the composition of the alkali-activated binder promotes its rapid setting, the formation of C–A–S–H phase with a low Al content, and AFm type phases in small quantities. Bernal, S.A. and Haha, M.B. et al. determined [16, 20] that a C–A–S–H gel with a large substitution of Ca for Al is formed in the composition upon hydration of alkali-activated binders with a small MgO amount. Increasing the Al content in the C–A–S–H gel above a certain value leads to a deterioration in the physico-mechanical properties of composites with this structure. In another research [15] Haha, M.B. with colleagues found that the high content of Al₂O₃ in the slag composition increases the amount of Al₂O₃ in the hydrotalcite formed during the alkaline reaction, which subsequently leads to recrystallization and deterioration of the physico-mechanical properties of the composites.

The goal of the paper is to determine the effect of the mineral wool production waste (MWPW) chemical composition on the phase composition, structure, and physico-mechanical properties of geopolymers.

The following tasks were solved:

- the phase composition of the geopolymer samples made of MWPW was established using the of X-ray diffraction and thermal analyzing methods;
- the surface microstructure of the samples was studied using scanning electron microscopy method;
- the influence of the microstructure and phase composition of the composites on the values of their average density, compressive strength, water adsorption and water resistance has been established.

2. Methods

2.1. Materials

The main criterion for the chemical composition of mineral wool is the acidity modulus M_a , which is calculated according to the following formula:

$$M_a = \frac{\text{SiO}_2 + \text{Al}_2\text{O}_3}{\text{CaO} + \text{MgO}}, \quad (1)$$

where the numerator and denominator are the total contents of these oxides, % by weight.

Throughout the research, five types of MWPW with an acidity modulus from 1 to 2 were tested. The chemical composition of the waste is given in Table 1.

Table 1. Chemical composition of MWPW.

Comp. No	Chemical composition, % by weight.											
	CaO	SiO ₂	Al ₂ O ₃	MgO	Na ₂ O	K ₂ O	TiO ₂	Fe ₂ O ₃	MnO	SO ₃	P ₂ O ₅	
	2	3	4	5	6	7	8	9	10	11	12	
w1	40.995	36.336	10.306	8.201	1.058	0.883	0.815	0.547	0.295	0.248	0.033	
w2	25.284	41.135	10.655	11.556	1.951	0.875	1.287	5.753	0.263	0.094	0.091	
w3	26.228	41.800	13.257	11.412	1.171	0.383	0.297	2.392	0.227	0.277	0.013	
w4	25.451	40.548	15.421	9.358	2.163	0.456	0.741	4.615	0.183	0.130	0.012	
w5	19.772	46.362	11.249	8.565	1.967	1.082	1.131	7.739	0.156	0.091	0.139	

The end of the Table 1

Chemical composition, % by weight.							Ratio of oxides				
Cl	CuO	Cr ₂ O ₃	ZnO	Co ₃ O ₄	NiO	Loss on ignition	CaO/SiO ₂	Al ₂ O ₃ /SiO ₂	MgO/Al ₂ O ₃	M_a	
13	14	15	16	17	18	19	20	21	22	23	
0.026	0.014	0.013	0	0	0	0.230	1.128	0.284	0.796	0.948	
0	0.020	0.033	0.011	0.012	0.007	0.973	0.615	0.259	1.085	1.406	
0.009	0.010	0.096	0	0.008	0.024	2.396	0.627	0.317	0.861	1.463	
0.009	0.017	0.099	0.017	0.010	0.008	0.762	0.628	0.380	0.607	1.608	
0.004	0.015	0.040	0.005	0.014	0.014	1.655	0.426	0.243	0.761	2.033	

Granular NaOH dissolved in water was used as an alkaline activator. Mass fraction of the main substance is not less than 99.5 %.

2.2. Compositions and sample manufacturing technology

Alkali-activated binders and composites based on them were manufactured according to the following technology. Five types of MWPW (see Table 1 for chemical compositions) were dried to constant weight at a temperature of 105 °C. Then the waste was milled to a specific surface area from 125.12 to 377.23 m²/kg using the dry method and up to almost 1,500 m²/kg using the wet method. The water was poured into a working mixer with an alkaline activator (NaOH) previously dissolved in it. Ground MWPW were gradually loaded and mixed for 5–7 minutes. The water/slag (W/S) ratio allowed achieving equal fluidity of the mortar mix. Cube-shaped samples with a face of 20 mm were made from the resulting mixture by vibration molding. Samples in the molds were kept at a temperature of 50 °C and a relative humidity of at least 85 % for 5 hours. Then, samples outside the molds were steamed at atmospheric pressure according to the regime of 3+6+2 h at an isothermal heating temperature of 85±5 °C. The steamed products were dried to constant weight at a temperature of 30 °C and a relative humidity of not more than 50 %, after which further tests were carried out.

The compositions tested in the study are presented in Table 2.

Table 2. The compositions tested in the study.

Comp. No	Binder composition, %					NaOH	Dimensional indicators of waste		W/S ratio
	MWPW (see Table 1 for chemical composition)						Average particle diameter, μm	The specific surface of the powders, m ² /kg	
	w1	w2	w3	w4	w5				
C1	98	–	–	–	–	2			
C2	97	–	–	–	–	3	18.096	125.12	0.27
C3	96	–	–	–	–	4			
C4	–	98	–	–	–	2			
C5	–	97	–	–	–	3	6.605	342.79	0.287
C6	–	96	–	–	–	4			
C7	–	–	98	–	–	2			
C8	–	–	97	–	–	3	6.482	349.3	0.267
C9	–	–	96	–	–	4			
C10	–	–	–	98	–	2			
C11	–	–	–	97	–	3	14.962	151.33	0.357
C12	–	–	–	96	–	4			
C13	–	–	–	–	98	2			
C14	–	–	–	–	97	3	6.002	377.23	0.327
C15	–	–	–	–	96	4			
C16	98	–	–	–	–	2			
C17	97	–	–	–	–	3	1.533	1,476.94	0.303
C18	96	–	–	–	–	4			
C19	–	–	–	98	–	2			
C20	–	–	–	97	–	3	3.096	731.32	0.332
C21	–	–	–	96	–	4			

2.3. Analytical techniques

Geopolymer samples were tested using X ray diffraction (XRD), differential thermal (DTA) and thermogravimetric (DTG) analyses, as well as scanning electron microscopy (SEM):

– XRD of samples was carried out using an ARL X'tra diffractometer (Switzerland). Samples of hydrated alkali-activated binders were ground in an agate mortar with an agate pestle with acetone before passing through a sieve with a 90 μm screen opening. The diffraction patterns were recorded on CuK α_{1+2} radiation in the range of angles $2\theta = 4-70^\circ$ with a speed of 1.2 °/min, in increments of 0.02 °, integration time 1 sec. Using the Hanawalt method with the ICDD PDF-2 database, the qualitative phase composition of the samples was determined.

– DTA and DTG of samples was carried out using a TGA/DSC1 device (Switzerland). MWPW samples and hydrated alkali-activated binders were prepared as for the XRD. 0.025 g of the crushed sample was weighed to the nearest 0.0001 g and poured into an alundum crucible with a volume of 150 μl. Next, the sample was condensed by tapping the crucible on the table. The crucible was mounted on a holder and placed in an oven. The sample was heated from 30 to 1000 °C at a rate of 10 °C/min.

– surface SEM of geopolymer samples was carried out using a Quanta 200 i 3D device (USA) in the low vacuum mode (10⁻³ Pa) with 20 kV accelerating voltage and a working distance of 15 mm.

The average density and compressive strength of geopolymer samples was determined by testing at least 10 cube samples with a 20 mm face of each composition.

The water adsorption of the samples in percent by weight was determined by the ratio of water mass absorbed by the sample at full saturation to the dry sample mass.

Water resistance (W) of samples activated by NaOH MWPW was determined by the following formula:

$$W = \frac{R_{ws}}{R_d}, \quad (2)$$

where R_{ws} is the compressive strength of the samples after aging in water for 90 days;

R_d is the compressive strength of dried samples according to the method described in section 2.2.

3. Results and Discussion

3.1. X ray diffraction

The results of X ray diffraction analysis of MWPW samples after alkaline activation are presented in Figure 1.

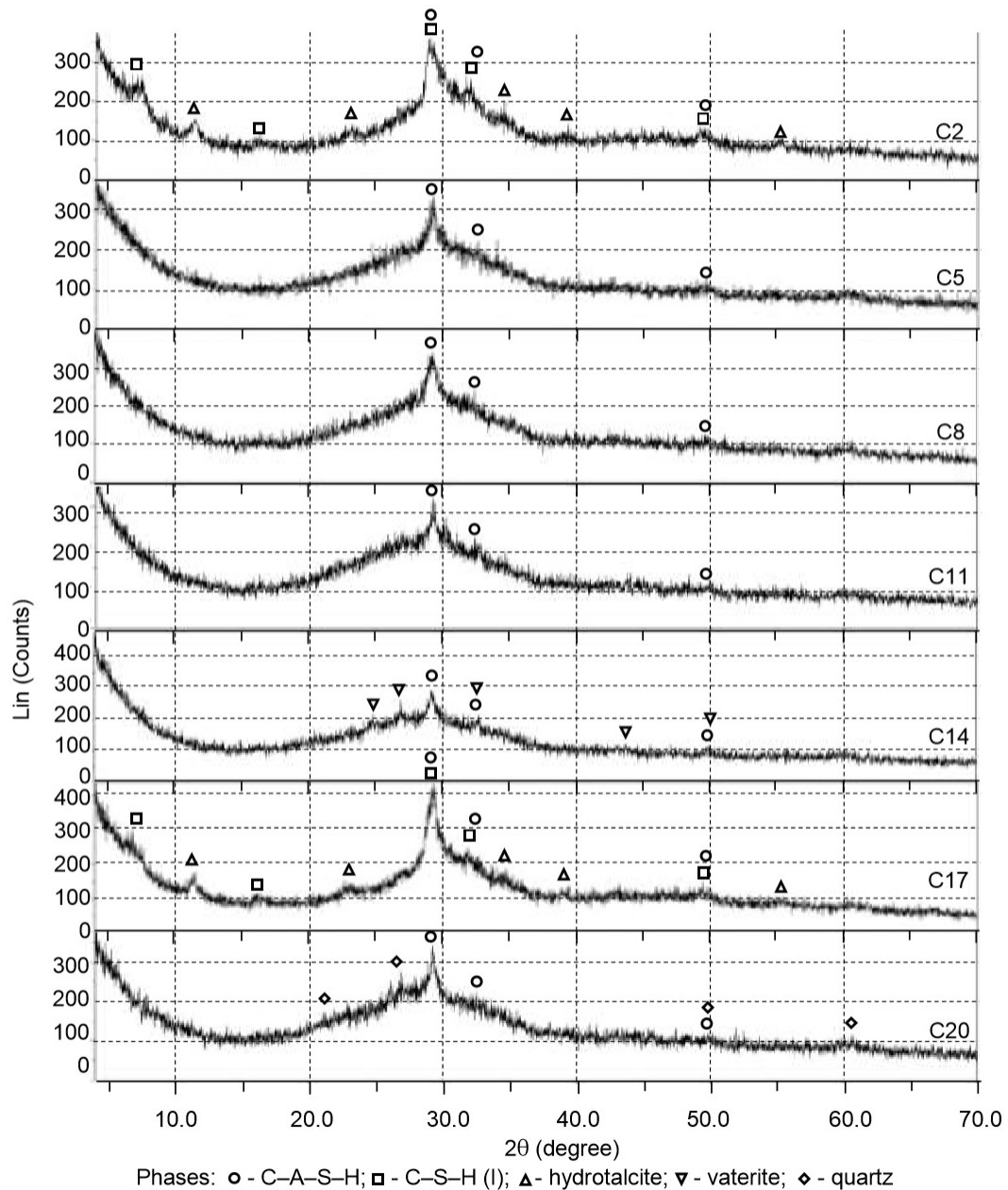


Figure 1. XRD samples of hydrated slag alkaline binders: C2, C5, C8, C11, C14, C17, C20 – see Table 2.

Definitive peaks for tobermorite-like calcium hydrosilicates with a partial replacement of Ca by Al C–A–S–H (PDF 00-033-0306) and C–S–H (I) (PDF 00-034-0002) were registered on X ray diffraction patterns of MWPW samples with an approximate CaO/SiO₂ ratio of 1.1, MgO/Al₂O₃ – 0.8 and Al₂O₃/SiO₂ – 0.3 (acid modulus M_a is approximately 1) after alkaline activation with an aqueous NaOH solution (compositions C2 and C17). Also, a significant amount of the secondary phase hydrotalcite (Mg₆Al₂(CO₃)(OH)₁₆·4H₂O, PDF 01-89-0460), was detected in the composition of these samples. An increase in the specific surface of the waste from 125.12 to almost 1,500 m²/kg led to a change in the X ray diffraction pattern of peak intensity at 2θ of about 29.5°, which indicates the formation of larger amounts of calcium hydrosilicates. The peaks on X ray diffraction patterns C2 and C17 related to hydrotalcite are almost identical, which indicates a slight effect of changes in the specific surface of the waste (from 125.12 to almost 1,500 m²/kg) on the formation of this phase.

The presence of peaks related to the C–A–S–H phase (PDF 00-033- 0306) was registered on X ray diffraction patterns C5 and C8 of hydrated alkali-activated binder samples made of MWPW with practically equal M_a (1.4–1.46) and CaO/SiO₂ ratio (0.6). The absence of secondary phases of the crystalline structure is determined. The main difference between these wastes lies in the MgO/Al₂O₃ ratio (about 0.26 for C5 and 0.32 for C8) and Al₂O₃/SiO₂ (about 0.26 for C5 and 0.32 for C8). Similar data was obtained by analyzing X ray diffraction patterns of activated NaOH waste with a M_a of about 1.6 and an equal CaO/SiO₂ and MgO/Al₂O₃ ratio of about 0.6 and Al₂O₃/SiO₂ of about 0.4 (compositions C11 and C20). Reflections related to quartz were additionally recorded on the X ray diffraction pattern C20 (PDF 00-046-1045), as well as an increase in peak intensity at 2θ of about 29.5°. An increase in the hydration degree of the C20 composition compared to C11.

X ray diffraction patterns of waste samples activated with NaOH with M_a of approximately 2 (composition C14) are characterized by the presence of peaks related to the C–A–S–H phase (PDF 00-033-0306), the absence of hydrotalcite peaks, and the occurrence of reflexes common for vaterite (PDF 00-024-0030).

3.2. Thermoanalysis

Thermoanalysis of the MWPW samples is presented in Figure 2 and in Table 3.

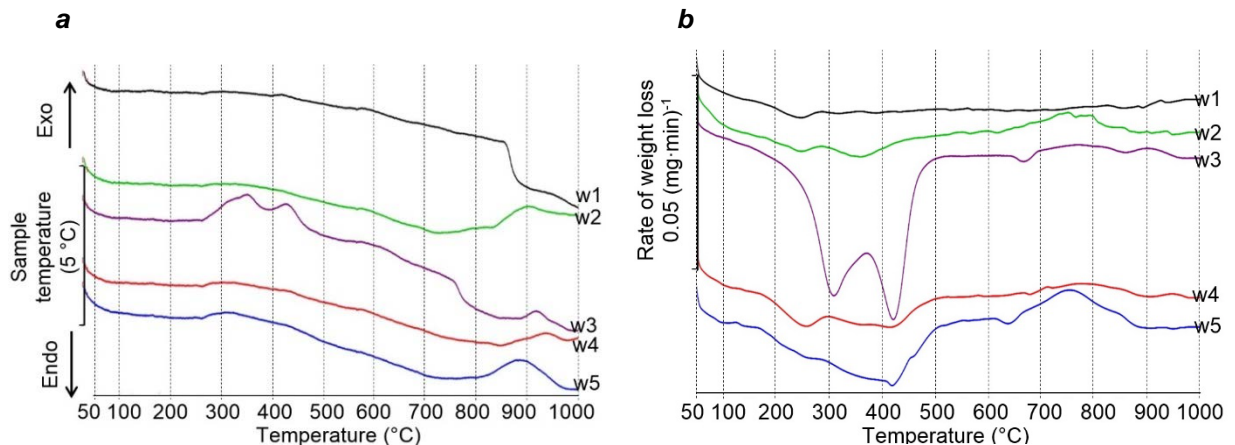


Figure 2. DTA (a) and DTG (b) MWPW curves: w1–w5 – see Table 1.

Table 3. Mass losses (in wt. %) of MWPW samples for various temperature ranges (°C).

Sample	30–250/°C	250–500/°C	500–600/°C	600–750/°C	750–1000/°C	30–1000/°C
w1	–0.099	–0.134	0.010	0.025	0.202	0.004
w2	–0.386	–0.585	–0.055	0.078	0.060	–0.888
w3	–0.083	–2.357	0.044	0.125	0.302	–1.969
w4	–0.183	–0.589	0.032	0.150	0.276	–0.314
w5	–0.486	–1.206	0.005	0.229	0.212	–1.246

According to the data obtained (Figure 2 and Table 3), the following main phase transformations occurring in the MWPW during heating were exposed. The first exothermic effect and sample mass loss in the temperature range from 250 to 500 °C corresponds to burning out of organic compounds used in bonding mineral wool to mats. The greatest mass loss and intensity of this effect are in the compositions w3 and w5. An insignificant endothermic effect with a peak at a temperature of about 570 °C without mass loss, observed on the DTA curves of all tested wastes, corresponds to the transition of β-quartz to α-quartz. The endothermic effect on the DTA curve (sample w3) at a temperature between 750 and 800 °C (the sample mass has not changed) corresponds to a softening of the glass phase in the waste. The exothermic effect with a peak at a temperature of about 850 °C, which was registered on the DTA curve w1, without mass loss by the sample refers to wollastonite crystallization. This exothermic effect for w2–w5 compositions is shifted to the area of

higher temperatures (peaks with maxima from 880 to 920 °C), which corresponds to the crystallization of melilite minerals. The results obtained correlate with the data of many researchers [2, 15–18, 22, 25, 27].

Thermoanalysis of geopolymer samples made of MWPW is presented in Figure 3 and in Table 4.

Table 4. Mass losses (wt. %) of geopolymers samples in various temperature ranges (°C).

Sample	30–250/°C	250–500/°C	500–600/°C	600–750/°C	750–1000/°C	30–1000/°C
C2	-6.560	-2.120	-0.319	-0.270	-0.120	-9.389
C5	-13.375	-2.049	-0.241	-0.180	0.040	-15.805
C8	-12.861	-3.561	-0.217	-0.163	0.097	-16.705
C11	-6.770	-2.206	-0.292	-0.347	0.126	-9.489
C14	-13.640	-2.057	-0.240	-0.136	0.171	-15.902
C17	-13.393	-2.677	-0.332	-0.256	-0.020	-16.678
C20	-17.760	-2.282	-0.347	-0.316	0.007	-20.698

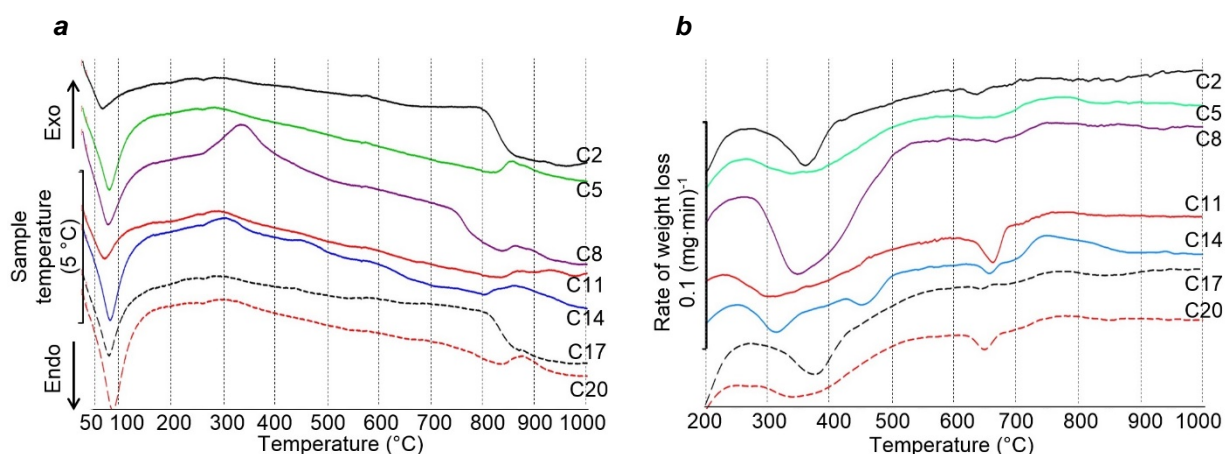


Figure 3. DTA (a) and DTG (b) curves of geopolymer samples: C2, C5, C8, C11, C14, C17, C20 – see Table 2.

According to the data presented in Table 4 and Figure 3, the main phase transformations during heating, occurring in hydrated alkaline-activated binder samples made of MWPW are as follows. The large endothermic effect on the DTA curves and the significant weight loss by all samples in the temperature range from 30 to 250 °C are associated with the dissociation of crystalline unbound water and the dehydration of calcium hydrosilicates. The presence of calcium hydrosilicates in all the samples is also indicated by the shift of exothermic effects with peaks at temperatures from 850 to 950 °C (Figure 2, a) to lower temperatures (Figure 3, a). The exothermic effect for compositions C2 and C17 with a peak at a temperature of about 810 °C is associated with crystallization of wollastonite made of calcium hydrosilicates with a CaO/SiO₂ ratio of approximately 1. The peak of this exothermic effect in the other compositions is shifted to the 860–870 °C temperature range, which is explained by the content of C–A–S–H phase in the sample composition. The presence of the C–A–S–H phase in the composition of samples obtained by MWPW alkaline activation with M_a between 1.4 and 2 can also be determined by the wide depression in the DTG curves and the mass loss of the samples in the temperature range from 250 to 500 °C (Table 4 and Figure 3, b). In this temperature range, the organic compounds used for bonding mineral wool mats burnt out also. The reaction is accompanied by an exothermic effect in the DTA curves and mass loss of the samples.

A slight endothermic effect and almost equal weight loss of samples C2 and C17 in the temperature range from 300 to 430 °C confirm the XRD data on the insignificant effect of changes in the specific surface of the waste from 125.12 to 1,476.94 m²/kg on the formation of hydrotalcite.

A small endothermic depression in the TA curves of all compositions with a peak at about 570 °C corresponds to the transition of β -quartz to α -quartz. The depressions in the DTG curves for sample C14, accompanied by insignificant endothermic effects in the temperature range from 260 to 350 °C and from 420 to 490 °C, probably correspond to the dehydration of calcium hydroaluminates and hydrogranates.

The mass losses of the MWPW samples activated with NaOH with M_a from 1.6 to 2, as well as the distinct depressions in the DTG curves at the temperature of about 650 °C, are associated with the dehydration of sodium-calcium aluminosilicate hydrates. The reaction is accompanied by a slight endothermic effect. The area of this depression for compositions with $M_a = 1.6$ decreases with an increase in the specific surface of the waste. This is most likely caused by an increase in the amount of the C–A–S–H phase binding Al, which is required for the formation of sodium-calcium aluminosilicate hydrates.

In the DTA curve for composition C14, two endothermic effects are additionally observed with maxima at temperatures around 430 and 700 °C. The appearance of these effects is associated with the formation of vaterite. The presence of this phase confirms the mass loss and depression in the DTG curve in the temperature range from 650 to 750 °C, as well as the results of XRD.

3.3. SEM

Comparative surface microstructure characteristics of the geopolymer samples made of MWPW with M_a equal to 1 and 1.4 are presented in Figure 4.

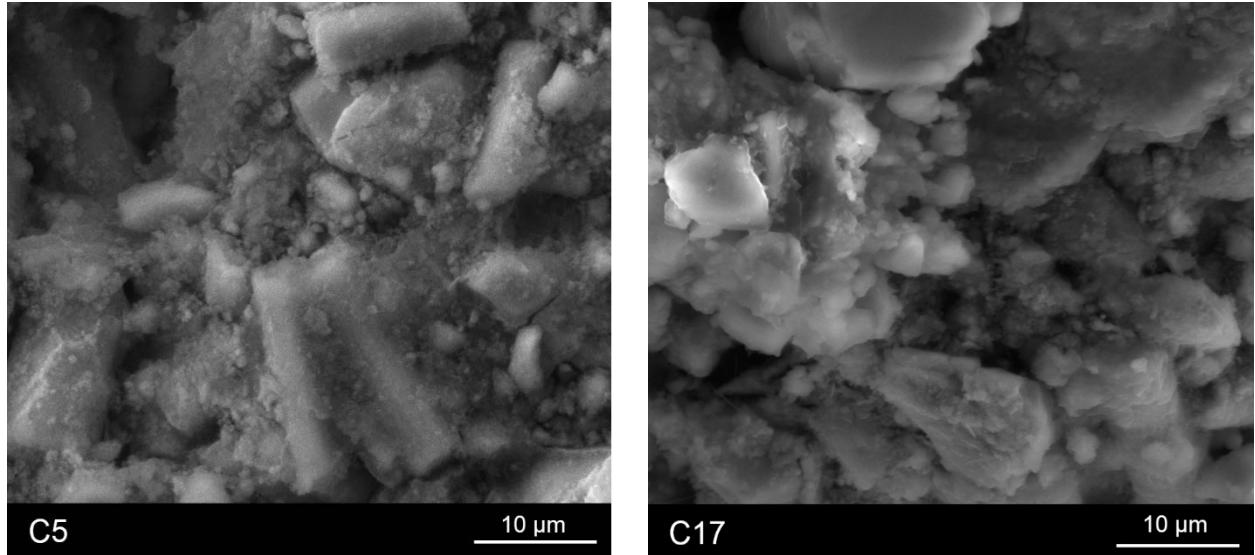


Figure 4. SEM-micrographs of geopolymer sample surfaces (compositions C5 and C17).

According to SEM-micrographs, the needle-shaped waste particles are visible on the surface of a geopolymer sample made of MWPW with $M_a = 1.4$ (C5). Almost the entire surface of the waste particles is covered with fibrous neoplasms, which most likely relate to tobermorite calcium hydrosilicates of C–A–S–H type. There are no clear boundaries between the particles. In the middle of Figure 4, the intergrowth of two needle-shaped particles of the C5 waste is clearly visible.

The microstructure of the geopolymer sample surface made of MWPW with $M_a = 1$ (C17) is as follows. The waste particles have a granular angular shape. Almost the entire surface of the particles is covered with neoplasms, mostly with a scaly structure, which is most likely relevant for the C–S–H (I) phase. Needle-shaped neoplasms representative for hydrotalcite crystals are also visible in the pores. In some places, neoplasms of the fibrous structure (C–A–S–H) are visible.

3.4. Average density and compressive strength

The average density values and compressive strength of geopolymer samples made of MWPW are presented in Figure 5.

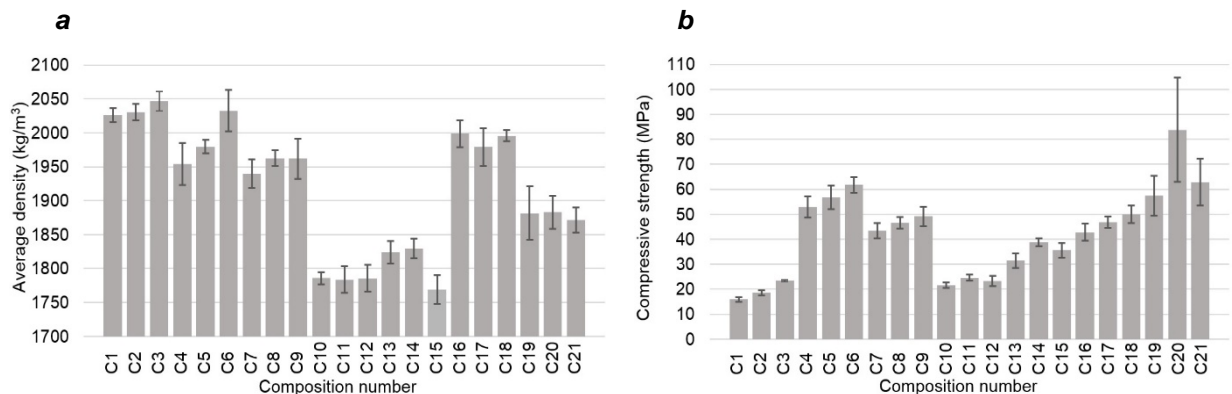


Figure 5. Average density (a) and compressive strength (b) of geopolymer samples.

While studying the hydration processes of MWPW activated with NaOH, it was found that only C1–C3 and C16–C18 compositions set and gain strength at a temperature of about 20 °C and a relative air humidity of at least 85 %. All compositions were obtained using MWPW with $M_a \approx 1$. The inability of the remaining compounds to self-set is associated with a low CaO content. This feature is described in the researches of

various authors [22, 25, 27]. It was previously determined [14], that geopolymer samples made of MWPW must be isothermally heated in molds for 5 hours at a temperature of at least 50 °C and a relative humidity of at least 85 %, in order to ensure the formwork strength. Based on these studies, a methodology for the manufacture of samples was developed, which is described in section 2.2. of the article.

Analyzing the average density values of the samples (Figure 5, a) allowed defining that this indicator decreases from 2,030 to about 1,800 kg/m³ on average with an increase of the waste M_a value from 1 to 2. Such an effect can be explained by a decrease in the true density of MWPW, as well as by the increase of the W/S ratio value of the mortar mixture.

According to the data (Figure 5, b), and also based on the results of previous studies [14], the compressive strength of geopolymer samples made of MWPW increases by 2.5–3 times with an increase in the waste M_a from 1 to 1.4. A further increase in the acid modulus to 2 leads to a decrease in compressive strength by almost 40%. In addition to M_a , the compressive strength of the samples depends on the specific surface of the waste. With an increase in the w1 specific waste surface from 125.12 to 1,476.94 m²/kg, the compressive strength of the samples increased by more than 2 times. An increase in the NaOH amount in the composition of the mortar mixture from 2 to 4 % slightly increases the compressive strength of the geopolymer MWPW samples with M_a between 1 and 1.46. Waste geopolymers with an acidity modulus of 1.6 and 2 have maximum compressive strength when activated with a 3 % NaOH.

The compressive strength of geopolymer samples is significantly affected by the Al₂O₃ content in the composition of MWPW. The effect is observed with an increase in the specific surface of the waste. The compressive strength values obtained for MWPW geopolymer samples with Al₂O₃ content of more than 15 % (w4) (specific waste surface is 731.32 m²/kg) were not stable. The spread between the maximum and minimum values of various samples was about 50 MPa, which is more than 40 % of the average value of this indicator. Such an effect was not observed when testing MWPW geopolymer samples with an Al₂O₃ content of about 10 %. Even with an increase in the specific surface of the waste to 1,500 m²/kg, the spread between the maximum and minimum compressive strength values of samples did not exceed 10 % of the average value.

3.5. Water absorption and water resistance

According to studies [2, 6, 14, 28, 29], the water resistance of geopolymers depends on the chemical composition of the initial slag. For example, glass-fiber composites with a CaO content of less than 6 % are not waterproof ($W < 0.8$), and NaOH-activated blast furnace slags continue to gain strength in water. The results of studies aimed at determining the water adsorption and water resistance of NaOH-activated MWPW samples with different acid modulus are presented in Figure 6.

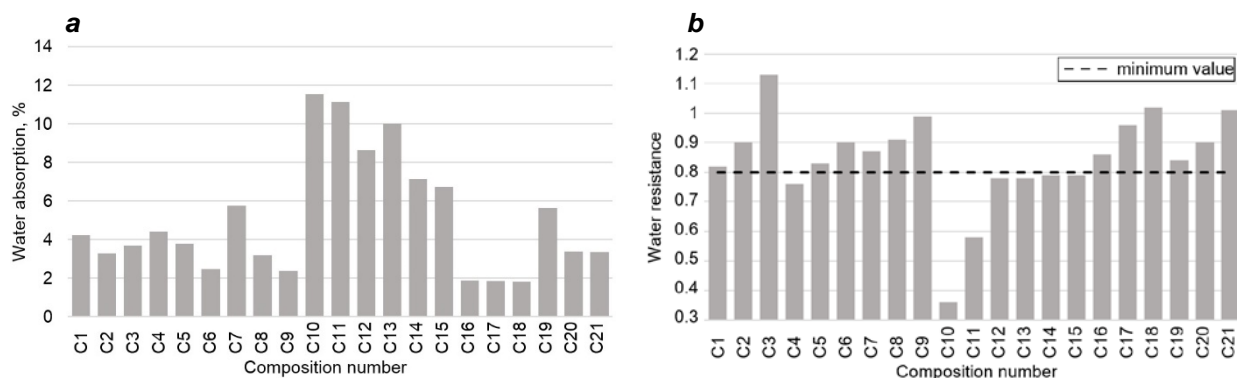


Figure 6. Water adsorption (a) and water resistance (b) of geopolymer samples.

According to the data obtained (Figure 6), the water adsorption of geopolymers depends on at least two following MWPW characteristics: chemical composition and fineness of grinding. The chemical composition of MWPW and the glue used in the preparation of mineral wool mats affect the amount of water required to obtain a mortar mixture of the equal mobility (W/S ratio). With an increase in the amount of water in the mortar mixture, the number of pores in the hardened composite increases. As a result, water adsorption increases. So, at almost equal specific MWPW surface area of the compositions w3 and w5, the W/S ratio of the mortar mixture is 0.06 lower for w3 waste (see Table 2), and the water adsorption of the hardened composite is almost 2 times less. Features of water adsorption by thermal insulation materials made of mineral wool are described in detail [30].

With increasing the MWPW specific surface, the W/S ratio of the mortar mixture increases, but the water adsorption of the hardened composite decreases. This feature can be explained by the filling of pores in the geopolymer with hydration products. According to XRD and TA data, NaOH-activated waste with a higher specific surface area has a greater degree of hydration. For example, when the specific surface area of w1 composition MWPW increases from 125.12 to 1,476.94 m²/kg, the W/S ratio of the mortar mixture increases from 0.27 to 0.303. At the same time, water adsorption of the geopolymer decreases by almost 2 times (from 3.8 to 1.9 % on average).

Resistance of MWPW geopolymers aged in water for 90 days depends on at least three following factors: the chemical composition of the waste, its specific surface, and the amount of alkaline component. With increasing M_a waste from 1 to 2, the water resistance of hardened composites decreases. For example, C8 geopolymers ($M_a = 1.46$) are water resistant ($W = 0.9$), and C14 ($M_a = 2$) are not waterproof ($W = 0.79$). It is possible to increase the water resistance of geopolymers by increasing the specific surface area of MWPW. Significant effect is achieved when using waste with $M_a > 1$. With an increase in the specific surface area of w4 waste composition from 377.23 (C11) to 731.32 m²/kg (C20), the samples of geopolymers became waterproof (water resistance increases from 0.58 to 0.9). An increase in the amount of alkaline component in the composition of the mortar mixture also increases the water resistance of the geopolymer. This effect decreases with increasing of waste M_a . So, with an increase of NaOH from 2 to 4 % in the composition of mortar mixture based on the waste w1 ($M_a = 1$), the water resistance increases from 0.82 to 1.13. However, it practically does not change if based on the w5 waste ($M_a = 2$) (W about 0.79).

4. Conclusion

1. The chemical composition impact of mineral wool production wastes (MWPW) on the phase composition, structure, and physico-mechanical properties of geopolymer samples has been determined.

2. It was defined using the methods of X ray differential and thermal analyses, that following tobermorite-like phases of calcium hydrosilicates are formed during hydration of NaOH-activated MWPW with $M_a = 1$: C–S–H (I) and C–A–S–H, as well as the secondary hydrotalcite phase. When waste M_a is activated from 1.4 to 2, neoplasms are represented mainly by the C–A–S–H phase. With an increase of M_a to more than 1.46, the presence of phases of sodium-calcium aluminosilicate hydrates, calcium hydroaluminates, and hydrogranates can also be detected in the geopolymer samples.

3. According to the SEM data, the C–A–S–H phase in the samples of hydrated MWPW with $M_a = 1.4$ has a fibrous structure, which covers almost the entire surface of the needle-shaped waste particles. Neoplasms in MWPW geopolymers with $M_a = 1$ are represented mostly by a scaly structure (probably the C–S–H (I) phase). In certain spots, needle-shaped neoplasms (hydrotalcite crystals) and fibrous structure (C–A–S–H phase) are observed.

4. It was established that the compressive strength of MWPW geopolymers samples strongly depends on the amount of the formed C–A–S–H phase of the fibrous structure. The water resistance of geopolymers is depends more on the amount of CaO in the initial waste composition. With its decrease, water resistance decreases. However, this indicator can be boosted by increasing the specific surface of the waste and by changing the amount of alkaline activator.

5. Water-resistant geopolymers (W is approximately 1) with a compressive strength of at least 80 MPa can be obtained by MWPW activation with 3–4 % of NaOH (in terms of dry matter). The acidity modulus of the waste should be in the range from 1.4 to 1.6, the Al₂O₃ content should be about 10 %, the specific surface area of at least 700 m²/kg.

6. The established regularities of structure formation processes of MWPW composites allow us to simulate their course in real conditions and select rational compositions of composites for use in specific areas of construction.

5. Acknowledgments

The work was carried out within the framework of the Grant of the President of the Russian Federation MK-6416.2018.3.

References

1. Bagheri, A., Nazari, A., Hajimohammadi, A., Sanjayan, J.G., Rajeev, P., Nikzad, M., Ngo, T., Mendis, P. Microstructural study of environmentally friendly boroaluminosilicate geopolymers. *Journal of Cleaner Production*. 2018. 189. Pp. 805–812. DOI: 10.1016/j.jclepro.2018.04.034.
2. Huseien, G.F., Sam, A.R.M., Shah, K.W., Asaad, M.A., Tahir, M.M., Mirza, J. Properties of ceramic tile waste based alkali-activated mortars incorporating GBFS and fly ash. *Construction and Building Materials*. 2019. 214. Pp. 355–368. DOI: 10.1016/j.conbuildmat.2019.04.154.
3. Kang, S.-H., Kwon, Y.-H., Hong, S.-G., Chun, S., Moon, J. Hydrated lime activation on byproducts for eco-friendly production of structural mortars. *Journal of Cleaner Production*. 2019. 231. Pp. 1389–1398. DOI: 10.1016/j.jclepro.2019.05.313.
4. Provis, J.L., Bernal, S.A. Geopolymers and related alkali-activated materials. *Annual Review of Materials Research*. 2014. 44. Pp. 299–327. DOI: 10.1146/annurev-matsci-070813-113515.
5. Provis, J.L., Palomo, A., Shi, C. Advances in understanding alkali-activated materials. *Cement and Concrete Research*. 2015. 78. Pp. 110–125. DOI: 10.1016/j.cemconres.2015.04.013.
6. Rafeet, A., Vinai, R., Soutsos, M., Sha, W. Effects of slag substitution on physical and mechanical properties of fly ash-based alkali activated binders (AABs). *Cement and Concrete Research*. 2019. 122. Pp. 118–135. DOI: 10.1016/j.cemconres.2019.05.003.
7. Erofeev, V., Korotaev, S., Bulgakov, A., Tretiakov, I., Rodin, A. Getting Fired Material with Vitreous Binder Using Frame Technology. *Procedia Engineering*. 2016. 164. Pp. 166–171. DOI: 10.1016/j.proeng.2016.11.606.

8. Fediuk R.S., Lesovik V.S., Svintsov A.P., Mochalov A.V., Kulichkov S.V., Stoyushko N.Y., Gladkova N.A., Timokhin R.A. Self-compacting concrete using pretreated rice husk ash. *Magazine of Civil Engineering*. 2018. 79(3). Pp. 66–76. DOI: 10.18720/MCE.79.7.
9. Heah, C.Y., Kamarudin, H., Mustafa Al Bakri, A.M., Bnhussain, M., Luqman, M., Khairul Nizar, I., Ruzaidi, C.M., Liew, Y.M. Study on solids-to-liquid and alkaline activator ratios on kaolin-based geopolymers. *Construction and Building Materials*. 2012. 35. Pp. 912–922. DOI: 10.1016/j.conbuildmat.2012.04.102.
10. Liew, Y.-M., Heah, C.-Y., Li, L.-Y., Jaya, N.A., Abdullah, M.M.A.B., Tan, S.J., Hussin, K. Formation of one-part-mixing geopolymers and geopolymer ceramics from geopolymer powder. *Construction and Building Materials*. 2017. 156. Pp. 9–18. DOI: 10.1016/j.conbuildmat.2017.08.110.
11. Nematollahi, B., Sanjayan, J. Effect of different superplasticizers and activator combinations on workability and strength of fly ash based geopolymer. *Materials and Design*. 2014. 57. Pp. 667–672. DOI: 10.1016/j.matdes.2014.01.064.
12. Shang, J., Dai, J.-G., Zhao, T.-J., Guo, S.-Y., Zhang, P., Mu, B. Alternation of traditional cement mortars using fly ash-based geopolymer mortars modified by slag. *Journal of Cleaner Production*. 2018. 203. Pp. 746–756. DOI: 10.1016/j.jclepro.2018.08.255.
13. Xie, J., Wang, J., Rao, R., Wang, C., Fang, C. Effects of combined usage of GGBS and fly ash on workability and mechanical properties of alkali activated geopolymer concrete with recycled aggregate. *Composites Part B: Engineering*. 2019. 164. Pp. 179–190. DOI: 10.1016/j.compositesb.2018.11.067.
14. Erofeev, V.T., Rodin, A.I., Yakunin, V.V., Bogatov, A.D., Bochkina, V.S., Chegodajkin, A.M. Alkali-activated slag binders from rock-wool production wastes. *Magazine of Civil Engineering*. 2018. 82(6). Pp. 219–227. DOI: 10.18720/MCE.82.20.
15. Haha, M.B., Lothenbach, B., Le Saout, G., Winnefeld, F. Influence of slag chemistry on the hydration of alkali-activated blast-furnace slag – Part II: Effect of Al_2O_3 . *Cement and Concrete Research*. 2012. 42(1). Pp. 74–83. DOI: 10.1016/j.cemconres.2011.08.005.
16. Haha, M.B., Lothenbach, B., Le Saout, G., Winnefeld, F. Influence of slag chemistry on the hydration of alkali-activated blast-furnace slag – Part I: Effect of MgO. *Cement and Concrete Research*. 2011. 41(9). Pp. 955–963. DOI: 10.1016/j.cemconres.2011.05.002.
17. Ismail, I., Bernal, S.A., Provis, J.L., San Nicolas, R., Hamdan, S., Van Deventer, J.S.J. Modification of phase evolution in alkali-activated blast furnace slag by the incorporation of fly ash. *Cement and Concrete Composites*. 2014. 45. Pp. 125–135. DOI: 10.1016/j.cemconcomp.2013.09.006.
18. Myers, R.J., Bernal, S.A., San Nicolas, R., Provis, J.L. Generalized structural description of calcium-sodium aluminosilicate hydrate gels: The cross-linked substituted tobermorite model. *Langmuir*. 2013. 29(17). Pp. 5294–5306. DOI: 10.1021/la4000473.
19. Tänzer, R., Buchwald, A., Stephan, D. Effect of slag chemistry on the hydration of alkali-activated blast-furnace slag. *Materials and Structures/Materiaux et Constructions*. 2014. 48(3). Pp. 629–641. DOI: 10.1617/s11527-014-0461-x.
20. Bernal, S.A., San Nicolas, R., Myers, R.J., Mejía De Gutiérrez, R., Puertas, F., Van Deventer, J.S.J., Provis, J.L. MgO content of slag controls phase evolution and structural changes induced by accelerated carbonation in alkali-activated binders. *Cement and Concrete Research*. 2014. 57. Pp. 33–43. DOI: 10.1016/j.cemconres.2013.12.003.
21. Geng, G., Myers, R.J., Li, J., Maboudian, R., Carraro, C., Shapiro, D.A., Monteiro, P.J.M. Aluminum-induced dreierketten chain cross-links increase the mechanical properties of nanocrystalline calcium aluminosilicate hydrate. *Scientific Reports*. 2017. 7. Article number 44032. DOI: 10.1038/srep44032.
22. Li, C., Sun, H., Li, L. A review: The comparison between alkali-activated slag (Si + Ca) and metakaolin (Si + Al) cements. *Cement and Concrete Research*. 2010. 40(9). Pp. 1341–1349. DOI: 10.1016/j.cemconres.2010.03.020.
23. Marsh, A., Heath, A., Patureau, P., Evernden, M., Walker, P. Alkali activation behaviour of un-calcined montmorillonite and illite clay minerals. *Applied Clay Science*. 2018. 166. Pp. 250–261. DOI: 10.1016/j.clay.2018.09.011.
24. Ogundiran, M.B., Kumar, S. Synthesis and characterisation of geopolymer from Nigerian Clay. *Applied Clay Science*. 2015. 108. Pp. 173–181. DOI: 10.1016/j.clay.2015.02.022.
25. Walkley, B., San Nicolas, R., Sani, M.-A., Rees, G.J., Hanna, J.V., van Deventer, J.S.J., Provis, J.L. Phase evolution of C-(N)-A-S-H/N-A-S-H gel blends investigated via alkali-activation of synthetic calcium aluminosilicate precursors. *Cement and Concrete Research*. 2016. 89. Pp. 120–135. DOI: 10.1016/j.cemconres.2016.08.010.
26. Węgrzyn, A., Rafalska-Lasocha, A., Majda, D., Dziembaj, R., Papp, H. The influence of mixed anionic composition of Mg-Al hydrotalcites on the thermal decomposition mechanism based on in situ study. *Journal of Thermal Analysis and Calorimetry*. 2010. 99(2). Pp. 443–457. DOI: 10.1007/s10973-009-0190-5.
27. Garcia-Lodeiro, I., Aparicio-Rebollo, E., Fernández-Jimenez, A., Palomo, A. Effect of calcium on the alkaline activation of aluminosilicate glass. *Ceramics International*. 2016. 42(6). Pp. 7697–7707. DOI: 10.1016/j.ceramint.2016.01.184.
28. Erofeev, V.T., Fedortsov, A.P., Bogatov, A.D., Fedortsov, V.A., Gusev, B.V. Evaluation of corrosion of alkaliglass composites, predicting their physico-chemical resistance and ways to improve it. *Proceedings of Higher Education Institutions: Textile Industry Technology*. 2018. 374(2). Pp. 238–246.
29. Hanjitsuwan, S., Phoo-ngernkham, T., Li, L.-Y., Damrongwiriyanupap, N., Chindapasirt, P. Strength development and durability of alkali-activated fly ash mortar with calcium carbide residue as additive. *Construction and Building Materials*. 2018. 162. Pp. 714–723. DOI: 10.1016/j.conbuildmat.2017.12.034.
30. Vatin, N.I., Pestryakov, I.I., Sultanov, Sh.T., Ogidan, T.O., Yarunicheva, Y.A., Kiryushina, A.P. Water vapour by diffusion and mineral wool thermal insulation materials. *Magazine of Civil Engineering*. 2018. 81(5). Pp. 183–192. DOI: 10.18720/MCE.81.18.

Contacts:

Vladimir Erofeev, +7(8342)47-40-19; a_l_rodin@mail.ru
 Alexander Rodin, +7(951)051-45-28; a_l_rodin@mail.ru
 Vladislav Yakunin, +7(953)029-70-58; vladisjakunin@yandex.ru
 Maksim Tuvin, +7(987)691-35-09; maxim.tuvin@yandex.ru

© Erofeev, V.T., Rodin, A.I., Yakunin, V.V., Tuvin, M.N., 2019



DOI: 10.18720/MCE.90.1

Структура, состав и свойства геополимеров из отходов минеральной ваты

В.Т. Ерофеев, А.И. Родин*, В.В. Якунин, М.Н. Тувин

Мордовский государственный университет им. Н.П. Огарёва, г. Саранск, Республика Мордовия, Россия

* E-mail: al_rodin@mail.ru

Ключевые слова: геополимеры, отходы, минеральная вата, механические свойства, рентгенофазовый анализ, термический анализ, микроструктура

Аннотация. При производстве минеральной ваты образуются отходы в количестве до 30 % от массы готовой продукции. Данные отходы можно использовать при изготовлении строительных материалов, в частности в качестве сырья для получения геополимеров (шлакощелочных вяжущих). Цель исследования состояла в установлении влияния химического состава отходов производства минеральной ваты (ОПМВ) на фазовый состав, структуру и физико-механические свойства геополимеров. Пять видов ОПМВ с различным химическим составом и удельной поверхностью гидратировали в присутствии NaOH (от 2 до 4 мас. %). Экспериментальные результаты получены с применением методов рентгенофазового (РФА), дифференциально-термического (ДТА) и дифференциально-термогравиметрического (ДТГ) анализа, сканирующей электронной микроскопии (СЭМ), физико-механических испытаний. Установлено, что основным продуктом гидратации ОПМВ в присутствии NaOH являются гидросиликаты кальция типа C–A–S–H волокнистой структуры. Наибольшее количество C–A–S–H зафиксировано в образцах геополимеров из отходов с модулем кислотности от 1,4 до 1,6. Прочность при сжатии полученных материалов достигает 80 МПа. Они также характеризуются высокой водостойкостью. Для получения геополимеров со стабильными свойствами содержание Al_2O_3 в отходе должно быть около 10 %. Выявленные результаты позволили установить взаимосвязь между структурой, составом и физико-механическими свойствами геополимеров из ОПМВ. Практическая значимость результатов исследования заключается в возможности получения бетонов более высоких классов по прочности.

Литература

1. Bagheri A., Nazari A., Hajimohammadi A., Sanjayan J.G., Rajeev P., Nikzad M., Ngo T., Mendis P. Microstructural study of environmentally friendly boroaluminosilicate geopolymers // *Journal of Cleaner Production*. 2018. 189. Pp. 805–812. DOI: 10.1016/j.jclepro.2018.04.034.
2. Huseien G.F., Sam A.R.M., Shah K.W., Asaad M.A., Tahir M.M., Mirza J. Properties of ceramic tile waste based alkali-activated mortars incorporating GBFS and fly ash // *Construction and Building Materials*. 2019. 214. Pp. 355–368. DOI: 10.1016/j.conbuildmat.2019.04.154.
3. Kang S.-H., Kwon Y.-H., Hong S.-G., Chun S., Moon J. Hydrated lime activation on byproducts for eco-friendly production of structural mortars // *Journal of Cleaner Production*. 2019. 231. Pp. 1389–1398. DOI: 10.1016/j.jclepro.2019.05.313.
4. Provis J.L., Bernal S.A. Geopolymers and related alkali-activated materials // *Annual Review of Materials Research*. 2014. 44. Pp. 299–327. DOI: 10.1146/annurev-matsci-070813-113515.
5. Provis J.L., Palomo A., Shi C. Advances in understanding alkali-activated materials // *Cement and Concrete Research*. 2015. 78. Pp. 110–125. DOI: 10.1016/j.cemconres.2015.04.013.
6. Rafeet A., Vinai R., Soutsos M., Sha W. Effects of slag substitution on physical and mechanical properties of fly ash-based alkali activated binders (AABs) // *Cement and Concrete Research*. 2019. 122. Pp. 118–135. DOI: 10.1016/j.cemconres.2019.05.003.
7. Erofeev V., Korotaev S., Bulgakov A., Tretiakov I., Rodin A. Getting Fired Material with Vitreous Binder Using Frame Technology // *Procedia Engineering*. 2016. 164. Pp. 166–171. DOI: 10.1016/j.proeng.2016.11.606.
8. Федюк Р.С., Лесовик В.С., Свинцов А.П., Мочалов А.В., Куличков С.В., Стоюшко Н.Ю., Гладкова Н.А., Тимохин Р.А. Самоуплотняющийся бетон с использованием предварительно подготовленной золы рисовой шелухи // *Инженерно-строительный журнал*. 2018. № 3(79). С. 66–76. doi: 10.18720/MCE.79.7
9. Heah C.Y., Kamarudin H., Mustafa Al Bakri A.M., Bnhussain M., Luqman M., Khairul Nizar I., Ruzaidi C.M., Liew Y.M. Study on solids-to-liquid and alkaline activator ratios on kaolin-based geopolymers // *Construction and Building Materials*. 2012. 35. Pp. 912–922. DOI: 10.1016/j.conbuildmat.2012.04.102.
10. Liew Y.-M., Heah C.-Y., Li L.-Y., Jaya N.A., Abdullah M.M.A.B., Tan S.J., Hussin K. Formation of one-part-mixing geopolymers and geopolymer ceramics from geopolymer powder // *Construction and Building Materials*. 2017. 156. Pp. 9–18. DOI: 10.1016/j.conbuildmat.2017.08.110.

11. Nematollahi B., Sanjayan J. Effect of different superplasticizers and activator combinations on workability and strength of fly ash based geopolymer // *Materials and Design*. 2014. 57. Pp. 667–672. DOI: 10.1016/j.matdes.2014.01.064.
12. Shang J., Dai J.-G., Zhao T.-J., Guo S.-Y., Zhang P., Mu B. Alternation of traditional cement mortars using fly ash-based geopolymer mortars modified by slag // *Journal of Cleaner Production*. 2018. 203. Pp. 746–756. DOI: 10.1016/j.jclepro.2018.08.255.
13. Xie J., Wang J., Rao R., Wang C., Fang C. Effects of combined usage of GGBS and fly ash on workability and mechanical properties of alkali activated geopolymer concrete with recycled aggregate // *Composites Part B: Engineering*. 2019. 164. Pp. 179–190. DOI: 10.1016/j.compositesb.2018.11.067.
14. Ерофеев В.Т., Родин А.И., Якунин В.В., Богатов А.Д., Бочкин В.С., Чеодайкин А.М. Шлакощелочные вяжущие из отходов производства минеральной ваты // *Инженерно-строительный журнал*. 2018. № 6(82). С. 219–227. doi: 10.18720/МСЕ.82.20
15. Haha M.B., Lothenbach B., Le Saout G., Winnefeld F. Influence of slag chemistry on the hydration of alkali-activated blast-furnace slag – Part II: Effect of Al_2O_3 // *Cement and Concrete Research*. 2012. 42(1). Pp. 74–83. DOI: 10.1016/j.cemconres.2011.08.005.
16. Haha M.B., Lothenbach B., Le Saout G., Winnefeld F. Influence of slag chemistry on the hydration of alkali-activated blast-furnace slag – Part I: Effect of MgO // *Cement and Concrete Research*. 2011. 41(9). Pp. 955–963. DOI: 10.1016/j.cemconres.2011.05.002.
17. Ismail I., Bernal S.A., Provis J.L., San Nicolas R., Hamdan S., Van Deventer J.S.J. Modification of phase evolution in alkali-activated blast furnace slag by the incorporation of fly ash // *Cement and Concrete Composites*. 2014. 45. Pp. 125–135. DOI: 10.1016/j.cemconcomp.2013.09.006.
18. Myers R.J., Bernal S.A., San Nicolas R., Provis J.L. Generalized structural description of calcium-sodium aluminosilicate hydrate gels: The cross-linked substituted tobermorite model // *Langmuir*. 2013. 29(17). Pp. 5294–5306. DOI: 10.1021/la4000473.
19. Tänzer R., Buchwald A., Stephan D. Effect of slag chemistry on the hydration of alkali-activated blast-furnace slag. *Materials and Structures // Materiaux et Constructions*. 2014. 48(3). Pp. 629–641. DOI: 10.1617/s11527-014-0461-x.
20. Bernal S.A., San Nicolas R., Myers R.J., Mejía De Gutiérrez, R., Puertas, F., Van Deventer, J.S.J., Provis, J.L. MgO content of slag controls phase evolution and structural changes induced by accelerated carbonation in alkali-activated binders // *Cement and Concrete Research*. 2014. 57. Pp. 33–43. DOI: 10.1016/j.cemconres.2013.12.003.
21. Geng G., Myers R.J., Li J., Maboudian R., Carraro C., Shapiro D.A., Monteiro P.J.M. Aluminum-induced dreierketten chain cross-links increase the mechanical properties of nanocrystalline calcium aluminosilicate hydrate // *Scientific Reports*. 2017. 7. Article number 44032. DOI: 10.1038/srep44032.
22. Li C., Sun H., Li L. A review: The comparison between alkali-activated slag (Si + Ca) and metakaolin (Si + Al) cements // *Cement and Concrete Research*. 2010. 40(9). Pp. 1341–1349. DOI: 10.1016/j.cemconres.2010.03.020.
23. Marsh A., Heath A., Patureau P., Evernden M., Walker P. Alkali activation behaviour of un-calcined montmorillonite and illite clay minerals // *Applied Clay Science*. 2018. 166. Pp. 250–261. DOI: 10.1016/j.clay.2018.09.011.
24. Ogundiran M.B., Kumar S. Synthesis and characterisation of geopolymer from Nigerian Clay // *Applied Clay Science*. 2015. 108. Pp. 173–181. DOI: 10.1016/j.clay.2015.02.022.
25. Walkley B., San Nicolas R., Sani M.-A., Rees G.J., Hanna J.V., van Deventer J.S.J., Provis J.L. Phase evolution of C-(N)-A-S-H/N-A-S-H gel blends investigated via alkali-activation of synthetic calcium aluminosilicate precursors // *Cement and Concrete Research*. 2016. 89. Pp. 120–135. DOI: 10.1016/j.cemconres.2016.08.010.
26. Węgrzyn A., Rafalska-Lasocha A., Majda D., Dziembaj R., Papp H. The influence of mixed anionic composition of Mg-Al hydrotalcites on the thermal decomposition mechanism based on in situ study // *Journal of Thermal Analysis and Calorimetry*. 2010. 99(2). Pp. 443–457. DOI: 10.1007/s10973-009-0190-5.
27. Garcia-Lodeiro I., Aparicio-Rebollo E., Fernández-Jimenez A., Palomo A. Effect of calcium on the alkaline activation of aluminosilicate glass // *Ceramics International*. 2016. 42(6). Pp. 7697–7707. DOI: 10.1016/j.ceramint.2016.01.184.
28. Ерофеев В.Т., Федорцов А.П., Богатов А.Д., Федорцов В.А., Гусев Б.В. Оценка коррозии стеклощелочных композитов, прогнозирование их физико-химического сопротивления и способы его повышения // *Известия высших учебных заведений: Технология текстильной промышленности*. 2018. № 2(374). Pp. 238–246.
29. Hanjitsuwan S., Phoo-ngernkham T., Li L.-Y., Damrongwiriyanupap N., Chindaprasit P. Strength development and durability of alkali-activated fly ash mortar with calcium carbide residue as additive // *Construction and Building Materials*. 2018. 162. Pp. 714–723. DOI: 10.1016/j.conbuildmat.2017.12.034.
30. Ватин Н.И., Пестряков И.И., Султанов Ш.Т., Огидан О.Т., Яруничева Ю.А., Кирюшина А. Диффузионное влагопоглощение теплоизоляционных изделий и минеральной ваты // *Инженерно-строительный журнал*. 2018. № 5(81). С. 183–192. doi: 10.18720/МСЕ.81.18.

Контактные данные:

Владимир Трофимович Ерофеев, +7(8342)47-40-19; эл. почта: al_rodin@mail.ru
Александр Иванович Родин, +7(951)051-45-28; эл. почта: al_rodin@mail.ru
Владислав Васильевич Якунин, +7(953)029-70-58; эл. почта: vladisjakunin@yandex.ru
Максим Николаевич Тувин, +7(987)691-35-09; эл. почта: maxim.tuvin@yandex.ru

© Ерофеев В.Т., Родин А.И., Якунин В.В., Тувин М.Н., 2019